Journal of Hazardous Materials, 20 (1988) 109-135
Elsevier Science Publishers B.V., Amsterdam - Printed in The Netherlands

ASSESSMENT OF MATHEMATICAL MODELS FOR FIRE AND EXPLOSION HAZARDS OF LIQUEFIED PETROLEUM GASES

W.P. CROCKER AND D.H. NAPIER
Department of Chemical Engineering and Applied Chemistry, 200 College Street, University of Toronto, Toronto, (Canada) M5S 1A4

SUMMARY

Models of fires and explosions from releases of LPG have been reviewed and modified to enable levels of thermal radiation and overpressure to be predicted. All of the releases considered were from pressurised storage.

Radiation and impingement effects from jet fires were estimated for quiescent and windy conditions. Correlations have been set down for thermal radiation from fireballs both at ground-level and in a rising, dynamic system. Blast effects of BLEVE's have been quantified on the basis of isentropic, adiabatic expansion of the LPG and of the TNT model for this energy source; the corresponding fireball was considered.

Comparison between candidate models was undertaken and the physical effects have been calculated. These values were set against damage criteria in order to allow specification of safety separation distances, which were then compared with recommended distances in safety codes.

Flash fires and UVCE's have also been discussed briefly.

From this study models have been recommended for various applications after appropriate modifications to satisfy physical requirements and to allow use of the correlations on a personal computer.

INTRODUCTION

The development of mathematical models of fires and explosions of liquefied petroleum gases (LPG) should enable safer designs to be produced and more adequate contingency plans to be formulated. The ranges of thermal radiation, blast and missiles can be computed thereby leading to values for safety separation distances. These distances are often at variance with codes and standards (1) which may incorporate some consideration of the likelihood of the event.

Mathematical models of fires and explosions vary considerably in the account that is taken of the physical and chemical aspects of the combustion system. The detail of the fuel source in relation to rate and magnitude of release have sometimes received inadequate attention.

Thus in order to optimise on the effort expended, models must be chosen with care in order to meet the specific requirement. Furthermore approximations are made in the formulation of models. An appreciation of these is necessary to enable the predicted values to be used to the best advantage.

Although the models may not directly depend upon the type of storage involved, the consequences of the event to which the model is applied, will so do. In this paper, the models considered are set down as applied to unrefrigerated i.e., pressurised, storage. The types of fire and explosion that can be produced will be reviewed briefly.

Modes of failure of LPG containers

This topic is a matter of importance in fire and explosion modelling in that it defines the source term i.e. the rate and magnitude of release of LPG from containment. The general types of failure for pressurised LPG containers are listed here:

(1) catastrophic: (a) failure by impact at low temperature;
(b) stress corrosion cracking.
(2) mechanical overpressurisation e.g. during LPG transfer.
(3) pierced in collision or excavation.
(4) effect of heat: (a) release from relief valve;
(b) failure of steel shell;
(c) overpressurisation of unrelieved vessel.

FIRES AND EXPLOSIONS OF LPG

The type of event that occurs depends upon:

(1) the nature and particularly the position of the failure on the vessel
(2) the rate of release
(3) rate of admixture with air
(4) proximity of sources of ignition

The resulting event may be one of the following

Fires: Jet, Flash or Fireball

Explosion: BLEVE or UVCE

There is the lesser likelihood of a pool or of a tank fire. The most favourable circumstances for these would be with a catastrophic or major butane release in a cold climate. Pool and tank fires have been considered in detail elsewhere (1) and because of their improbability they will only receive passing mention here.

Aspects of flames

Depending upon the position and degree of admixture of fuel and air, the type of flame produced will vary from turbulent diffusion to premixed. The constituents of LPG have considerable soot-forming propensity, so that the flames are likely to be strongly luminous. Flame luminosity also depends upon the efficiency of mixing with air. From these considerations, values for

emissivity must be inserted in the fire models selected for use. A value of unity may be assumed to produce conservative predictions of separation.

Flame temperature is also required when the Stefan-Boltzmann equation is used. There is a paucity of information on this topic for large flames. Jet flames may have temperatures approaching adiabatic values (2) but the assumption of a homogeneously radiating flame for diffusion systems is patently unsatisfactory. However, it is usual to employ such average values in that adequate data and methods of prediction are not available.

DAMAGE CRITERIA

The assessment of the impact that hazards from LPG have on their environs must be coupled with pertinent damage criteria. Of these thermal radiation is the major hazard from fires of LPG; severe damage to both people and property may occur. It is desirable to predict such damage; in this connection damage criteria are appropriate. Criteria have been recommended by Robertson (3) and in safety codes (4).

When the controlling parameters of the combustion system cause a significant temporal change in the radiant flux received at a target, the dosage summed over the exposure time must be addressed (5).

LPG can become involved in explosions (BLEVE and UVCE) which have numerous consequences (8). Appropriate personal injury criteria (9) due to overpressure and those for damage to buildings (9) and items of plant (10) have been described.

MATHEMATICAL MODELLING OF MAJOR HAZARDS

The main features of the models which are used to predict the magnitude of the impact from the hazard will be discussed; pertinent details of the models will be given.

Jet fires

Jet fires form as a pressurised torch fire when LPG escapes from a breach in containment. Two hazards associated with jet fires are: flame impingement and thermal radiation. The models presented here are used to predict the distribution of thermal radiation surrounding the flame (i.e. the radiation field). Flames formed in both quiescent and windy, turbulent atmospheres are considered in this paper.

Jet fires (quiescent atmosphere)

According to Tunc and Venart (11), the jet fire formed in a quiescent atmosphere is conical in form and involves lift-off.

The length of the flame, L, was based on the Hawthorne correlation (12) viz.

$$\frac{L-a}{d_j} = \frac{5.3}{C_T}\sqrt{\frac{T_f}{\alpha_T T_j}\left[C_T - (1 - C_T)\frac{M_a}{M_j}\right]} \quad (1)$$

The following assumptions were made for the model runs:

(1) critical flow conditions exist at either the relief valve or the breach during discharge.

(2) lift-off occurs and the flame burns at a distance above the port where the average velocity is 0.2 M (13).

An estimate of lift-off was made by invoking the model of the turbulent momentum jet (14).

$$a = \frac{U_j}{2\,U_\ell \tan\alpha}\sqrt{\frac{P_j M_j}{Z_P R T_j \rho_a}} \quad (2)$$

An alternate equation (13) for lift-off distance is,

$$a = 1.6\,\pi\,d_j \cdot \frac{v_o}{U_\ell} \quad (3)$$

Eqns. (2) and (3) were compared with measurements reported by Tunc and Venart (11) for an engulfed LPG rail car. The results in Table 1 indicate that eqn. (2) showed better agreement than eqn. (3).

TABLE 1

Comparison of lift-off predictions ($\alpha = 20°$; $d_j = 0.08$ m)

	Lift-off Distance (m)
Tunc/Venart (11)	4
Kent Correlation (eqn. 3)	2
Eqn. (2)	3.3

Having established the geometry of the flame, the appropriate view factor is required to predict the intensity of radiation, q, at the target using the Stefan-Boltzmann equation. Atmospheric attenuation has been neglected in this paper but methodologies are available to estimate atmospheric transmissivity (15).

Equations for the view factor, F, are given here based on the orientation of the target. These are derived from Becker's (16) integral equations; Simpson's Rule was used to integrate eqns. (4) and (5).

Horizontal Target

$$F = \frac{2}{\pi}\int_h^{h+L} \frac{\left[x \sin\psi + (z \tan\alpha - r_f)\psi\right] r_f z\,dz}{\left[x^2 + z^2\right]^2} \quad (4)$$

Vertical Target

$$F = \frac{2}{\pi}\int_h^{h+L} \frac{(x - r_f) r_f \left[x \sin\psi + (z \tan\alpha - r_f)\psi\right] dz}{\left[x^2 + z^2\right]^2} \quad (5)$$

in which the flame differential is located by its radius r_f and angular position ψ. These parameters are given by

$$r_f = [z-h] \tan \alpha + 0.5\, d_j \tag{6}$$

$$\psi = \cos^{-1} (r_f/x) \tag{7}$$

An analytical equation developed by Minning (17) can be used to predict radiant intensities at horizontal targets. The view factor is given by

$$F = \frac{w}{2\pi} + \frac{\sin \alpha}{\pi} \left\{ \tan^{-1}\left[H\sqrt{\frac{1 + \tan^2\alpha}{x^2 - S^2 \tan^2\alpha}}\right] - \tan^{-1}\left[S\sqrt{\frac{1 + \tan^2\alpha}{x^2 - S^2 \tan^2\alpha}}\right]\right\}$$

$$+ \frac{(H-S)^2 \tan^2\alpha - x^2 - H^2}{\pi\sqrt{(H-S)^2 \tan^2\alpha + x^2 + H^2]^2 - 4x^2(H-S)^2 \tan^2 \alpha}} \cdot \tan^{-1}\left[\left[\frac{((H-S) \tan \alpha + x)^2 + H^2}{((H-S) \tan \alpha - x)^2 + H^2}\right.\right.$$

$$\left.\left. \cdot \left(\frac{x + S \tan \alpha}{x - S \tan \alpha}\right)\right]^{1/2}\right] \tag{8}$$

in which $w = \cos^{-1} \left(-\frac{S \tan \alpha}{x}\right)$

$S = h - z_t$

$H = L + h - z_t$

Separation distances should determined using these relations by considering maximum thermal emissions which occur at two-thirds along the flame axis (18,19). Eqn. 5 cannot be modified to accommodate this and was used with the target datum at the apex of the cone.

In the above, buildings and people are modelled as vertical targets while in-ground storage and low level plant constitute horizontal targets. Orientation of targets is of importance in specifying spacing distances for people. If the separation distances are based on the horizontal target (2), the required distance would be too small. As shown in Fig. 1, vertical targets receive radiation from the fire well into the far field.

As shown in Fig. 2, the radiation field surrounding the jet fire is strongly dependent on the semi-angle α which controls the area and orientation of the radiating "surface".

Choice of view factor is always an important feature of modelling. Two view factors (eqns. (4) and (8)) were compared for the cone and the horizontal target. At low values of α, the view factors (eqns. (4) and (8)) show reasonable agreement but as the angle α increases, the Minning view factor predicts the higher value. This is shown in Fig. 3.

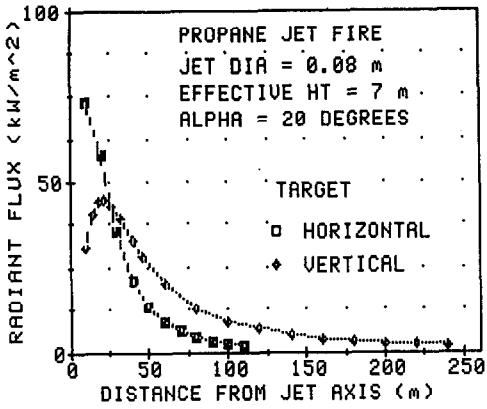

Fig. 1. Effect of target orientation on radiation field

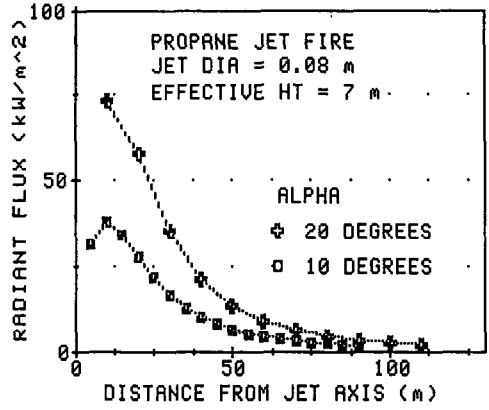

Fig. 2. Effect of conical semi-angle on radiation field (horizontal target)

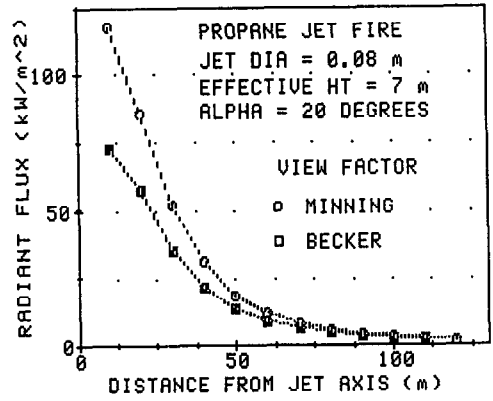

Fig. 3. Effect of view factor on radiation field (horizontal target)

Jet fires (windy atmosphere)

Wind causes the flame to tilt downwind extending the radiation and impingement hazards. Models have been developed based on different representations of the flame. Correlations to size the flame are based on small-scale experiments in wind tunnels. The details of these models are presented here.

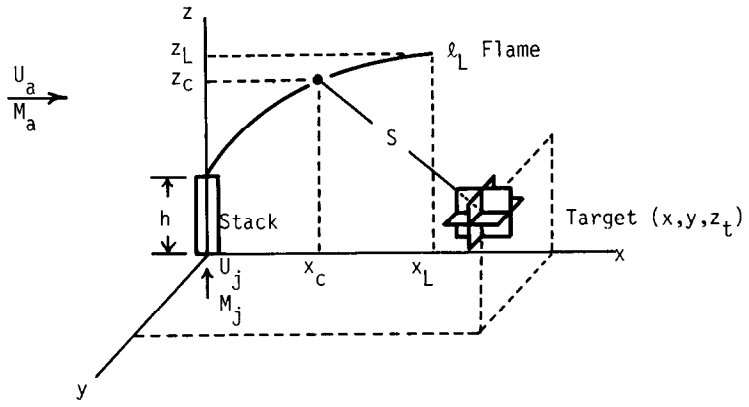

Fig. 4. PS model of tilted jet fire

Point source (PS) model. The flame correlations were based on cold flow studies of the dispersion of hydrocarbon jets in a cross-wind (20). The equation for the axis of the flame is

$$\bar{z} = 2.05(\bar{x})^{0.28} \tag{9}$$

Dimensional and non-dimensional parameters for distance are related by

$$z = \bar{z}\, d_j r \tag{10}$$

$$x = \bar{x}\, d_j r \tag{11}$$

in which $r = \dfrac{U_j\sqrt{\rho_j}}{U_a\sqrt{\rho_a}}$

The so-called dimensionless lower flammable limit, $\bar{c}_L$, is defined by

$$\bar{c}_L = c_L \frac{U_j}{U_a} \cdot \frac{M_j}{M_a} \tag{12}$$

The following set of equations is used to calculate the dimensionless vertical height of the flame tip, $\bar{z}_L$, above the exit.

When $\bar{c}_L < 0.5$,

$$\bar{\ell}_L = \frac{2.04}{(\bar{c}_L)^{1.03}} \tag{13}$$

$$\bar{x}_L = \bar{S}_L - 1.65 \tag{14}$$

and when $\bar{c}_L \geq 0.5$,

$$\bar{\ell}_L = \frac{2.51}{(\bar{c}_L)^{0.625}} \tag{15}$$

but if $\bar{\ell}_L > 2.35$, then

$$\bar{x}_L = \bar{\ell}_L - 1.65 \tag{16}$$

and if $\bar{\ell}_L \leq 2.35$, then

$$\bar{\ell}_L = 1.04\ \bar{x}_L^{\,2} + 2.05\ \bar{x}_L^{\,0.28} \tag{17}$$

Eqn. (17) is solved for $\bar{x}_L$ which is substituted into equation (9) for $\bar{z}_L$. Thereby the geometry of the flame is established.

The model is based on the concept of combustion occurring at a point source located centrally between 0 and x_L. The intensity of radiation, q, at any target in space can be calculated from

$$q = \frac{fQ \cos \beta}{4\pi S^2} \tag{18}$$

Equations developed to predict, q, at the targets shown in Fig. 4 are given by the following:

Horizontal Target

$$q = \frac{fQ(z_c - z_t)}{4\pi S^3} \tag{19}$$

Vertical Target (perpendicular to x-axis)

$$q = \frac{fQ(x - 0.5\ x_L)}{4\pi S^3} \qquad (x \quad 0.5\ x_L) \tag{20}$$

Vertical Target (parallel to x-axis)

$$q = \frac{fQ\ y}{4\pi S^3} \tag{21}$$

in which $S^2 = (z_c - z_t)^2 + y^2 + (x - 0.5\ x_L)^2$

$z_c = 0.823\ z_L + h$

$Q = \pi/4\ d_j^{\,2}\ U_j\ \Delta H_c$

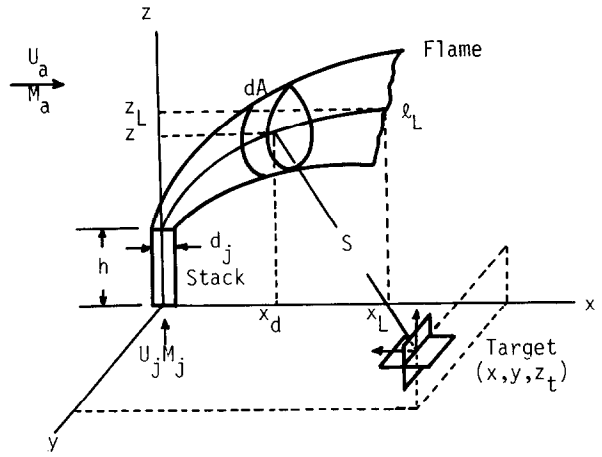

Fig. 5. MPS model of jet fire

Multiple point source (MPS) model. The total intensity of radiation, q, received at the target for the jet fire system shown in Fig. 5 is given by

$$q = \int_A \frac{\varepsilon\sigma T_f^4 \cos\beta \, dA}{4\pi S^2} \qquad (22)$$

in which $dA = 2\pi x_d^{0.4} (d_j r)^{0.6} d\ell$

This results in

$$q = \frac{\varepsilon\sigma T_f^4}{2} (d_j r)^{0.6} \int_0^{\ell_L} \frac{x_d^{0.4} \cos\beta \, d\ell}{S^2} \qquad (23)$$

The geometry of the flame must be determined before q can be calculated. Correlations were developed from wind tunnel studies of methane and LPG burning in small "flares" (21). The correlation range is U_j/U_a between 0 and 76. Equations describing the flame in Fig. 5 are given by the following semi-empirical correlations (22):

$$\bar{\ell}_L = \frac{3.8}{(\bar{c})^{0.48}} \quad \text{for } \bar{c}_L \leq 0.5 \qquad (24)$$

$$\bar{\ell}_L = \frac{3.9}{(\bar{c}_L)^{0.60}} \quad \text{for } \bar{c}_L > 0.5$$

The downwind position, $\bar{x}_L$, of the flame tip is given by

$$\bar{\ell}_L = 3.2 \, \bar{x}_L^{0.54} \qquad (26)$$

The equation of the flame axis which describes the vertical height, z, of the flame differential, is given by

$$z = 3.1 \, x_d^{0.36} (d_j r)^{0.64} + h \qquad (27)$$

The intensity of radiation, q, can be calculated by numerically integrating eqn. (23) by the Simpson's Rule. Based on the orientation of the target, the following definitions for cos β are required for the calculation

Horizontal Target

$$\cos \beta = \frac{z - z_t}{S} \qquad (z_t < h) \tag{28}$$

Vertical Target

$$\cos \beta = \frac{x - x_d}{S} \qquad (x > x_L) \tag{29}$$

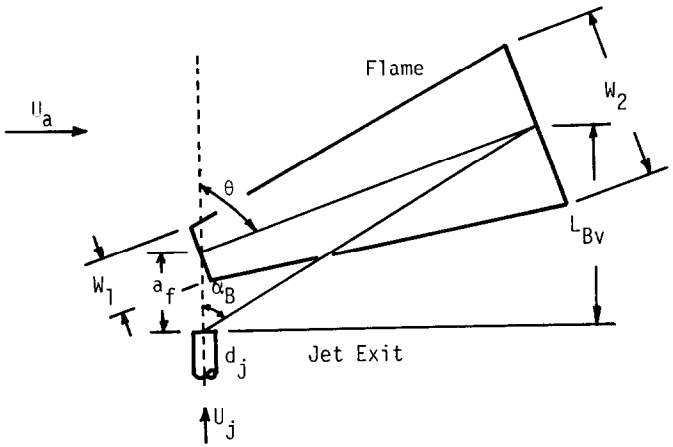

Fig. 6. SF model of tilted jet fire

Solid flame (SF) model of jet fire. Kalghatgi (23) developed correlations to describe the geometry of the windblown jet shown in Fig. 6. The correlations are given by the following equations

$$\alpha_B = 94 - \frac{1.6}{R_v} - 35\ R_v \qquad \text{(degrees)} \tag{30}$$

$$\theta = 94 - \frac{1.1}{R_v} - 30\ R_v \qquad \text{(degrees)} \tag{31}$$

$$\frac{L_{BV}}{D_S} = 6 + \frac{2.35}{R_v} + 20\ R_v \tag{32}$$

$$\frac{W_2}{D_S} = 80 - \frac{0.57}{R_v} - 570\ R_v + 1470\ R_v^2 \tag{33}$$

$$\frac{W_1}{D_S} = 49 - \frac{0.22}{R_v} - 380\ R_v + 950\ R_v^2 \tag{34}$$

when $R_v = \frac{U_a}{U_j}$

$$D_S = d_j \sqrt{\frac{\rho_j}{\rho_a}}$$

Computation of the view factor for the jet fire shown in Fig. 6 requires that the geometry of a tilted cylinder of equivalent area be defined (24). The diameter, D_e, of this cylinder is

$$D_e = 2 \sqrt{\frac{W_1+W_2}{L}} \left[L^2 + (W_2-W_1)\right]^{1/4} \quad (35)$$

and the flame length, L, of the cylinder can be developed using the dimensions in Fig. 7.

$$L = \frac{L_{BV} \sin \alpha_B}{\sin (90-\alpha_B) \sin (180-\theta)} \quad (36)$$

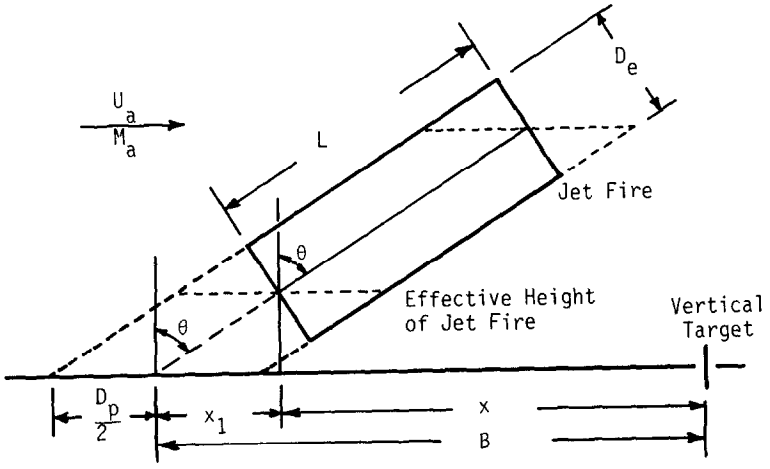

Fig. 7. Equivalent cylinder model of tilted jet fire

The virtual exit of the jet fire is located at a distance, a_f, from the jet exit (Fig. 6).

$$a_f^2 = L^2 + L_B^2 - 2 L L_B \cos (\alpha-\alpha_B) \quad (37)$$

when $L_B = \frac{L_{BV}}{\sin (90-\alpha_B)}$

The intensity of radiation, q, can be calculated at the target shown in Fig. 7. The view factor F for a tilted cylinder has been described elsewhere (1, 25-26).

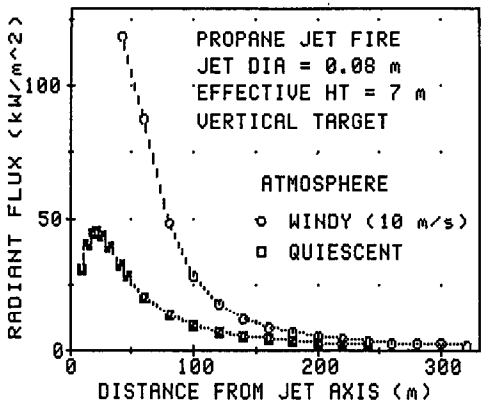

Fig. 8. Effect of wind on radiation field

TABLE 2

Separation distances from propane jet fire burning at vent

(Jet: dia.=0.08 m, height=4m, pressure=1.93 MPa, temp.=328 K)

Model	Wind Velocity (ms^{-1})	x_L	z_L	ℓ_L	a	Separation distances (m) to radiation level (kWm^{-2}) 12.6	4.7	1.6
Becker (α=20°)	0	0	0	26	3	82	143	250
SF model (tilted)	10	34	32	38	12	135	201	318
MPS model (tilted)								
[f=1]	10	19	45	46	0	326	601	1173
[f=.33]	10	19	45	46	0	166	306	596
PS model (tilted)								
[f=.33]	10	13	24	32	0	65	111	189

Discussion of jet fire models

The results of a comparison between the models of the jet fire are given in Table 2. Wind in this system causes the extension of the radiation hazard by tilting the flame downwind and by causing the flame to lengthen (Fig. 8). The lack of agreement between the results in Table 2 is noteworthy. This stems from the fact that each model is based on its own set of premises from small-scale experiments. Hence the derived geometry and size of the wind-blown flame is different in each case. Thus, assessment of the models must be on the basis of

the original premises, assumptions in the development, ease of manipulation and degree of validation.

In the context of these criteria, the SF model is based on acceptable geometry from which a physically-sound model can be developed. Thus both the radiation incident upon targets and the impingement distances are acceptable. Further reason for preference of the SF model is that the correlations used to define the flame geometry are based on the largest scale of validation. However, uncertainty is introduced by the use of a cylinder to represent the frustrum; the validity of this assumption must await radiation measurements.

COMBUSTION OF VAPOUR CLOUDS

When LPG is released from containment without immediate ignition, the fluid flashes due to its superheated condition. Thereby a vapour cloud is formed with a significant amount of entrained mist. The direction and shape of this heavy gas cloud (by virtue of molecular weight and low temperatures) is dependent on the size and location of the breach in containment.

The hazard developed by combustion of the cloud is dependent on the location of the source of ignition and the degree of admixture with the surrounding air. The principal hazards from vapour clouds are:

Flash Fire

Fireball

Unconfined Vapour Cloud Explosion.

These hazards will be outlined briefly.

Flash fire

Perhaps the most common of the hazards is the flash fire which is associated with the burn-back of LPG vapour clouds. As the flammable vapour cloud disperses downwind, it may eventually encounter a source of ignition. The flame travels back towards the source through premixed regions of the cloud. When the vapour cloud is not confined and free of obstacles, the progress of the band of flame is blast-free.

On this basis the estimation of consequences depends upon heavy gas dispersion modelling and the probability of ignition. It is usual to consider ignition at the 50% LFL isopleth but this may not incorporate the detail of actual dispersion or the likelihood of positive effects of ignition sources. It has also been customary to assume that only persons directly exposed to the flame will be killed. Acceptance of this rule of thumb may be misleading.

Analysis and modelling of flash fires has received little attention in spite of the fact that the hazard occurs frequently.

Considine (27) has outlined an approach for calculating the hazard ranges for people situated perpendicular and parallel to the direction of flame

propagation. Attention has also been directed to the problem by Raj (28), Croce and Mudan (24) and Eisenberg (29).

Fireballs

When the vapour cloud from flashing LPG encounters a source of ignition, the flame front propagates through the outer edges of the cloud without producing any significant overpressure. A large scale turbulent diffusion-type flame is formed when there is large fraction of the cloud above the upper flammable limit; intense thermal radiation is generated. The burning cloud expands and when it becomes buoyant, the fireball rises until burnout. However, in view of the fact that the gas is pressurised it usually rises due to its initial momentum.

Ground-level model of fireball

Traditionally, the fireball is modelled as a ground-level sphere whose maximum diameter is reached instantaneously and maintained during the period of combustion (30-32). Intensities of radiation, q, can be predicted at ground-level targets by the following equations.

Horizontal Target

$$q = \varepsilon\sigma T_f^4 \left(\frac{D}{2S}\right)^3 \qquad (38)$$

Vertical Target (people)

$$q = \varepsilon\sigma T_f^4 \frac{D^2 x}{4 S^3} \qquad (39)$$

Quantitative assessment of hazards to people and to buildings was made by assuming that exposure time is the same as the burning duration of the fireball. Intensities of radiation were used as damage criteria based on dosage values (5) for people. The maximum intensity of radiation received at the building (vertical target) is given by

$$q = \varepsilon\sigma T_f^4 \left(\frac{D}{2 S_B}\right)^2 \qquad (40)$$

and specification of safety zones for pilot and spontaneous ignition at the buildings is possible, by using the correlations of Lawson and Simms (6).

Results (Tables 3-5) are reported for the release of 50 tonnes of butane and of propane stored at ambient temperature (300 K). Upon release, the material is assumed to adiabatically flash (doubled to account for liquid entrainment (33)) and is in the fireball.

The correlations of Roberts (32) were used to estimate the fireball diameter, D, and the duration, t_d, as an effective source of radiation.

$$D = 5.8\ m^{1/3} \qquad (41)$$

$$t_d = 0.45\ m^{1/3} \qquad (42)$$

Propane fireballs are significantly more hazardous than butane fireballs; this involves considerations of flashing. The results in Table 3 indicate that buildings are exposed to ignition hazards (up to ½ km). The choice of the surface flux of the fireball is important. As shown in Table 5, different separation distances are predicted based on reasonable fluxes reported in the literature.

TABLE 3

Separation distances from ground-level fireball centerline to buildings

Roberts Correlations

Propane: $D = 187$ m $t_d = 14.5$ s $q_s = 340$ kWm^{-2} (24)

Butane: $D = 146$ m $t_d = 11.3$ s $q_s = 380$ kWm^{-2} (24)

Ignition hazard	Flux level (kWm^{-2}) propane	butane	Separation distances (m) propane	butane
Pilot	14.8	15	449	367
Spontaneous	26.2	26.4	337	277

TABLE 4

Separation distances from ground-level propane fireball ($q_s = 340$ kWm^{-2}) to buildings

(Vapour cloud) Roberts correlations: $D = 187$ m $t_d = 14.5$ s

(BLEVE) Maurer correlations: $D = 111.5$ m $t_d = 10$ s

Ignition hazard	Flux level (kWm^{-2}) Roberts VC	Maurer BLEVE	Separation distances (m) Roberts VC	Maurer BLEVE
Pilot	14.8	15.1	449	265
Spontaneous	26.2	26.4	337	200

TABLE 5

Separation distances for people from ground-level fireball (propane)

Roberts correlations: $D = 187$ m and $t_d = 14.5$ s

Damage	Flux level (kWm^{-2})	Fireball surface flux (kWm^{-2}) 450(32)	340(24)
1% lethality	25	379	325
50% lethality	44.7	273	230
Blistering	9.6	633	547
2nd degree burns	27.4	361	308
3rd degree burns	49	258	217

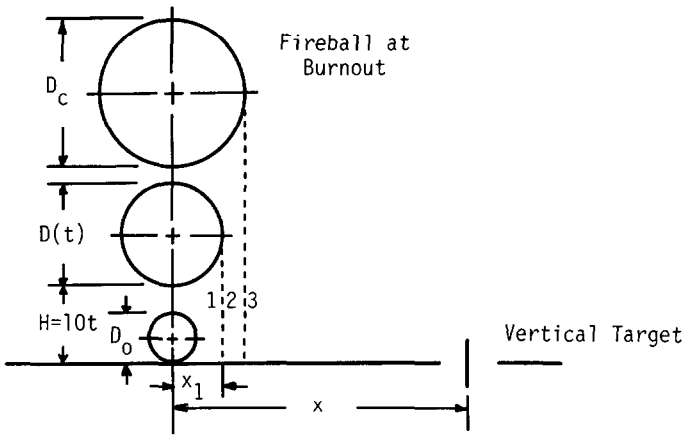

Fig. 9. Dynamic model of fireball

Dynamic fireball model

The model for isothermal fireballs developed by Lihou and Maund (34-35) was modified to incorporate the dynamics of the rising and expanding fireball. The modified model predicts the radiant dosage received at the vertical target. The computation is divided into three regions based on location of the target (Fig. 9). In an ambient temperature of 21°C, isothermal temperatures for propane and butane fireballs are 2085 and 1993 K respectively (36,34). These values are very close to the adiabatic flame temperature, thus a run was performed for propane at a significantly lower flame temperature viz 1678 K, surface flux 450 kWm^{-2}.

When the target is located at a distance less than the final fireball radius, the vertical axis of the target becomes tangential to the fireball at one point,

x_1, in the rise. The radiant flux, q, incident at the vertical ground target while the fireball is rising in region 1 is

$$q = \varepsilon\sigma T_f^4 F_1(t) \tag{43}$$

and $F_1(t)$, the view factor (37), is given by

$$F_1(t) = \left[\frac{D(t)}{2\,S}\right]^2 \frac{x_1}{S} \tag{44}$$

$$S^2 = [0.5\,D(t) + 10\,t]^2 + x_1^2 \tag{45}$$

When the radius of the fireball exceeds x_1, i.e. region 2, eqn. (44) is no longer valid because the vertical axis of the target intersects the sphere. The applicable view factor (38) becomes,

$$F_2(t) = \frac{-\sqrt{(L^2+H^2-1)(1-H^2)}}{\pi(L^2+H^2)} + \frac{1}{\pi}\tan^{-1}\sqrt{\frac{1-H^2}{L^2+H^2-1}}$$

$$- \frac{H}{\pi(L^2+H^2)^{3/2}} \cos^{-1}\frac{H\sqrt{L^2+H^2-1}}{L} \qquad (0 \leq x_1 < 0.5\,D(t)) \tag{46}$$

where $L = \dfrac{0.5\,D(t) + H(t)}{0.5\,D(t)}$

$H = \dfrac{-x_1}{0.5\,D(t)}$

The radiant dosage received at the target which is less than $D_c/2$, is given by

$$Q_d = 10^{-4}(\varepsilon\sigma T_f^4)^{4/3}\left[\int_0^{t_1}[F_1(t)]^{4/3}dt + \int_{t_1}^{t_d}[F_2(t)]^{4/3}dt\right] \tag{47}$$

The radiation calculation for region 3 (target location greater than final fireball radius) is identical to that for region 1, except that the exposure time is the burning time, t_d.

Computation of the radiant dosage is the more appropriate method to assess hazard in the light of the dynamic nature of the system. Separation distances are given in Table 6 for LPG's. As shown in Fig. 10, the location of the target is important because the distribution of the radiant flux is strongly dependent on time. The shape of the curves is dependent on the assumption that the fireball rise and the expansion are linear functions of time.

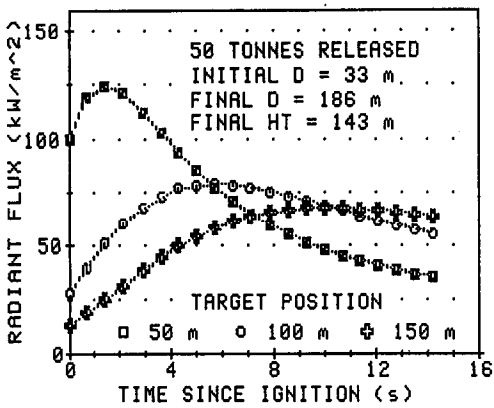

Fig. 10. Variation of radiation with time of combustion

TABLE 6

Distances from lift-off axis of fireball for various physiological effects
Dynamic fireball model: 50 tonnes released, Ambient temperature 300 K

Damage	Dosage $10^{-4}[s(Wm^{-2})^{4/3}]$	T_f(K):	Propane 2085	Propane 1678	Butane 1993
			Distances (m)		
1% lethality	1060		329	110	182
50% lethality	2300		196	N/A	70
Blistering	1200		696	376	428
2nd degree burns	2600		307	85	166
3rd degree burns	210-700		175	N/A	35

N/A = radiant dosage not obtained by target.

BLEVE

BLEVE is the physical explosion produced by the release of a superheated liquid to the atmosphere. In the context of LPG storage, the events leading to BLEVE's are well-defined (39,40). The release of energy from the pressure burst and the adiabatic flashing of the liquid into vapour produces a localised blast wave (41,43,44). For LPG release, immediate ignition is highly likely and it leads to a turbulent expanding fuel-air combustion system (fireball) which rises due to buoyancy. Thermal radiation from the fireball is the major hazard for an LPG BLEVE, but missiles, tub rocketing and the blast waves associated with the gas release are hazards to consider.

Blast effects of BLEVE's

A calculation is presented here which will give the theoretical maximum energy available to generate a blast wave (42,45,46). The following assumptions are made:

(1) the container holding the propane is a closed system (no relief is available);

(2) external source of heating raises the temperature and vapour pressure of the propane;

(3) failure of the vessel occurs when the internal pressure equals the rupture pressure;

(4) the initial volume of LPG stored as a liquid is set by its filling density at 60°F;

(5) the behaviour of the propane upon heating is described by its phase equilibrium (47);

(6) from thermodynamic considerations, the adiabatic expansion is isentropic and the energy for the resulting shock wave arises from the change in internal energy. The final state is a 2-phase system at atmospheric pressure and the normal boiling point.

The calculation is summarised as follows:

(1) calculation of the specific volume v;

$$v = \frac{V_c}{m} \tag{48}$$

(2) The state of the fluid at the point of rupture (v,P = rupture pressure) is established; s_2, E_2, T can be read from the tables (48);

(3) With isentropic expansion, $s_1 = s_2$, the final state of the fluid (2 phase) can be calculated;

$$s_2 = (1-x)s_{fg} + xs_g \quad \text{(at normal boiling point)} \tag{49}$$

$$u_1 = (1-x)u_{fg} + xu_g \tag{50}$$

(4) Energy available is $\Delta u = u_2 - u_1$

The TNT equivalent was calculated for adiabatic flash evaporation. By assuming the applicability of Hopkinson's scaling law (41), overpressure damage-distance quantities were determined using the data for TNT given by Briscoe and Shaw (8).

The results of the calculation (Table 7) illustrate the theoretical maximum hazards possible. The main difficulties in this approach are assumption of TNT-like behaviour and assignment of the explosive yield. The distances predicted based on the lower range of scaled distances show reasonable agreement with NFPA values.

TABLE 7

BLEVE overpressure calculations adiabatic flash evaporation at rupture pressure (59 bar), $\Delta u = -6829.8\ kJ \cdot kg^{-1}$

50 tonnes propane in tank (111.2 m^3)

Observed damage	Scaled distances	100% yield distances (m)	40% yield distances (m)
Limit serious structural damage	15.5	253	186
Limit minor structural damage	22.1	361	266
Missile limit	44.5	726	535
Broken glass damage	220	3591	2645

NFPA evacuation distance against tubs and missiles 762-914 m (49).

BLEVE fireball

The LPG container engulfed in fire is ruptured and the gas released is ignited (34). This leads to the formation of a highly turbulent rising fireball.

There is no general relationship that describes the rate of rise for the fireball (50,34) after lift-off. Croce and Mudan (24) developed a model for the rising fireball based on the details of the BLEVE at Cresent City.

The traditional approach to fireballs is to neglect the lift-off and to assume a ground-level fireball (50). The correlation of Maurer (51) can be used to establish the pertinent size and the duration. In light of the uncertainties involved in the rise of the fireball, the approach made by Lihou and Maund (34) was somewhat arbitrary and assumed a pseudo-steady state for the fireball located at a height equal to one-half its maximum diameter. This model was used in the calculation of hazard distances for people. The radiant flux, q, at the target was calculated by

Horizontal Target (34)

$$q = 0.25\ \varepsilon\sigma T_f^4 \left(\frac{D}{S}\right)^3 \qquad (51)$$

Vertical Target

$$q = 0.25\ \varepsilon\sigma T_f^4\ \frac{D^2 x}{S^3} \qquad (52)$$

where $S = \sqrt{D^2 + x^2}$

The correlations of Maurer (51) are given by

$$D = 3.44\ \left[\frac{44.8\ M}{m}\right]^{1/3} \qquad (53)$$

$$t_d = 0.31\left[\frac{44.8\ M}{m}\right]^{1/3} \quad (54)$$

Eqns. (53) and (54) were developed based on studies of bursting vessels of propylene.

Results of the BLEVE fireball runs are given in Table 8. The assumption of the fireball being located at a height equal to 1/2D greatly reduces the predicted separation distances. In light of the uncertainties involved regarding the lift-off, the ground-level fireball model is preferred. The effect of target orientation is also shown in this table. Values of separation distances for LPG BLEVE's are given in Table 9.

TABLE 8

BLEVE fireball model

50 tonnes propane released; Ambient temperature 300 K; q_s = 340 kWm^{-2}

Effect of lift-off and orientation of target on separation distances (tabulated)

Damage	Flux level (kWm^{-2})	Ground-level (vertical target)	Stationary height at 1/2 D (vertical)	(horizontal)
1% lethality	32.9	165	75	105
50% lethality	58.8	114	N/A	59
Blistering	13.2	275	245	175
2nd degree burns	36.1	157	N/A	98
3rd degree burns	64.5	107	N/A	N/A

N/A: flux level never obtained

TABLE 9

Separation distances from ground-level BLEVE fireball

Propane: D = 112 m t_d = 10 s q_s = 340 kWm^{-2}

Butane: D = 79 m t_d = 7 s q_s = 380 kWm^{-2}

Damage	Flux level (kWm^{-2}) propane	butane	Separation distances (m) propane	butane
1% lethality	32.9	42.5	165	103
50% lethality	58.8	75.9	114	73
Blistering	13.2	17.7	275	177
2nd degree burns	36.1	46.6	157	102
3rd degree burns	64.5	83.3	107	68

Unconfined vapour cloud explosion

Unconfined vapour cloud explosions (UVCE's) are caused by a deflagration of the vapour cloud that propagates through the "premixed cloud". The flame front accelerates to speeds on the order of 50-100 ms^{-1} which generate blast waves

that can cause overpressure damage beyond the limits of the vapour cloud. Conditions that appear to be necessary for the formation of a UVCE (52) include:

partial confinement due to buildings, structure, trees
time delay before ignition
composition of vapour cloud (~ premixed)
quantity of material released (a threshold of 5 tonnes)

UVCE's are not a common hazard in transportation system where the release of LPG is likely to meet an immediate source of ignition (from collisonal friction sparks, hot surfaces, local fire). It is more likely to occur in stationary storage vessels which release LPG thus forming a vapour cloud.

STANDARDS

There are frequent requirements for specification of safety separation distances between LPG tanks and items of plant and other structures. Advice (53) on these values is available from, e.g. industrial codes, regulatory authorities, insurance industry, corporate rules and codes.

The following standards were used in the assessment of separation from the storage of 50 tonnes LPG in a bullet (spacing distances are given in Table 10):

(1) American Petroleum Institute Standard 5210 (54)
(2) NFPA 58 - 1983 (55)
(3) Canadian Gas Association, CAN1-B149.2 (56)
(4) F.M. Recommendations (57)
(5) Institute of Petroleum Refining Safety Code (58)

TABLE 10

Recommended minimum spacing distances from standards
Water capacity of tank = 29380 U.S. gallon

Association	Distances (m) between LPG tank and Property lines/ buildings	Adjacent tanks	Flammable liquid tank
A.P.I.	15	1	3 *
N.F.P.A.	15	1.5	6
C.G.A.	15	3	6 *
F.M.	22.9	1.5	23
I.P.	15	1.5	15

* refers to centerline of dyke.

The values given in Table 10 lack agreement amongst themselves. Comparison of these values with those computed from the models discussed above indicate that either reassessment of the codes may be necessary or a fuller description of the implications of the values in Table 10 should be available.

CONCLUSIONS

1. Jet fires (quiescent atmosphere). The Becker view factor is adequate to predict the radiation hazard from the jet fire. Meaningful input data on the semi-angle α is required as the model runs showed that the radiation field is highly dependent on α. There is lack of agreement for view factors (cone with horizontal target); this discrepancy increases with increasing values of α.

2. Jet fires (windy atmosphere). The solid flame model based on the equivalent cylinder was the preferred candidate model; it is based on the largest scale of validation for the flame geometry.

3. Fireballs (vapour cloud). (a) the stationary ground-level fireball predicts greater safety distances when compared against a model developed to incorporate the rise and expansion of the fireball; (b) the dynamic model utilized a unique modification whereby the view factor for the vertical target directly beneath fireball was accounted for; (c) the rising fireball models show promise for future development.

4. BLEVE. (a) Blast effects were quantified. These results represented the theoretical maximum because the vessel was assumed to fail at the rupture pressure. Uncertainty is introduced by using the TNT model but improvement can be made by using a more detailed aerodynamic model; (b) the ground-level fireball is the preferred model in light of uncertainties in the rise of the BLEVE fireball.

NOMENCLATURE

a	lift-off distance	m
dA	differential area of flame	m^2
c_L	fractional LFL	
c_T	mole fraction of jet fluid in unreacted stoichiometric mixture	
d_j	diameter of jet	m
D	fireball diameter	m
D_c	final diameter of fireball	m
D_e	equivalent cylinder diameter	m
D_o	initial diameter of fireball	m
f	fraction of heat released as radiation	
F	view factor	
h	height of jet above ground	m
ΔH_c	net heat of combustion	kJ/kg
ℓ	distance from orifice along axis of jet	m
ℓ_L	arc length of flame centerline	m
L	visible flame length	m
L_{BV}	height of flame tip relative to jet exit	m
m	mass of fuel in fireball	kg

M_a	molecular weight of air	
M_j	molecular weight of jet fluid	
P_j	pressure at jet	Pa
q	intensity of radiation at target	kWm^{-2}
q(t)	intensity of radiation dependent on time	kWm^{-2}
q_s	surface flux of fireball	kWm^{-2}
Q	rate of heat release	kJ/s
Q_d	radiation dosage	$s(W/m^2)^{4/3}/10^4$
r_f	radius of flame at height z	m
R	universal gas constant	8.314 J/mol K
s	specific entropy	kJ/kg K
S_B	distance between fireball center and building	m
S	distance between point source and target	m
t	time after combustion	s
t_1	time when fireball meets target location x_1	s
t_d	duration of combustion	s
t_e	exposure time	s
T_f	flame temperature	K
T_j	temperature at jet	K
u	specific internal energy	kJ/kg
U_a	velocity of air	m/s
U_j	velocity of discharge from jet	m/s
U_ℓ	mean velocity of jet at distance ℓ	m/s
v	specific volume	m^3/kg
v_o	sonic velocity	m/s
V_c	volume of container	m^3
α	semi-angle of cone	degrees
α_T	ratio of reactants to products for stoichiometric mixture	
β	angle between normal and line joining point source and target	
ε	flame emissivity	
θ	flame tilt from vertical	degrees
ρ_a	density of air	kg/m^3
ρ_j	density of gas at jet	kg/m^3
σ	Stefan-Boltzmann constant	$5.67x10^{-11}$ kW/m^2K^4
ψ	angular position of flame differential	radians
x	position of target	m
$\bar{x}$	dimensionless downwind distance	m
x_d	downwind co-ordinate of flame differential	m
x_L	downwind distance of flame tip	m
y	cross-wind distance of target	m
z	height of flame differential	m

$\bar{z}$	dimensionless height above the exit on the centerline	
z_c	vertical position of point source	m
Z_p	compressibility factor	
z_t	target height above ground	m

REFERENCES

1 W.P. Crocker and D.H. Napier, Thermal radiation hazards of pool fires and tank fires, in: Hazards in the process industries: Hazards IX (I.Chem.E. Symp. Series No. 97), UMIST, Manchester, England, 1986, pp. 159-184.

2 A.D. Craven, Thermal radiation hazards from the ignition of emergency vents, in: I.Chem.E. Symp. Series No. 33, London, 1972, pp. 7-11.

3 R.B. Robertson, Spacing in chemical plant design against loss by fire, in: Proc. Symposium on Process Industry Hazards (I.Chem.E. Symp. Series No. 47), Livingston, Scotland, 1976, pp. 157-173.

4 Guide for Pressure - Relieving and Depressuring Systems, API Recommended Practice 521, 2nd edn., American Petroleum Institute, Washington, D.C., 1982.

5 I. Hymes, The physiological and pathological effects of thermal radiation, SRD R275, Safety and Reliability Directorate, UKAEA, 1983.

6 D.I. Lawson and D.L. Simms, The ignition of wood by radiation, Br. J. Appl. Phys., 3 (Sept. 1952), 288-292.

7 D.J. Rasbash, Review of explosion and fire hazard of liquefied petroleum gases, Fire Safety J., 2 (1979/80) 223-236.

8 W.C. Brasie and D.W. Simpson, Guidelines for estimating damage explosion, Loss Prevention, 2 (1968) 91-102.

9 J.A. Campbell, Estimating the magnitude of macro-hazards, Technology Report 81-2, Society of Fire Protection Engineers, Mass., 1981.

10 R.W. Nelson, Know your insurer's expectations, Hydrocarbon Processing, (Aug. 1977) 103-108.

11 M. Tunc and J.E.S. Venart, Incident radiation from a flare to a horizontal cylinder - Part II, Fire Safety J., 8 (1984/85) 89-96.

12 W.R. Hawthorne, D.S. Weddell and H.C. Hottel, Mixing and combustion in turbulent gas jets, 3rd Symposium in Combustion, Flame and Explosion Phenomena, Baltimore, Maryland, The Williams and Wilkens Co., 1949, pp. 266-288.

13 G.R. Kent, Find radiation effect of flares, Hydrocarbon Processing, 47(6) (1968) 119-130.

14 F.P. Lees, Loss prevention in the process industries, London, UK, Butterworth, 1980, pp. 461-462.

15 I.C. Simpson, Atmospheric transmissivity - the effects of atmospheric attenuation on thermal radiation, SRD R304, Safety and Reliability Directorate, UKAEA, 1984.

16 R. Becker, Mathematical model of luminous flame radiation for the determination of safety zones, Ger. Chem. Eng., 3 (1980) 229-233.

17 C.P. Minning, Calculation of shape factors between rings and inverted cones sharing a common axis, Trans. of ASME: J. Heat Transfer, 99 (August 1977) 492-494.

18 M. Law, Heat radiation from fires and building separation, Fire Research Technical Paper No. 5, HMSO, London, 1963.

19 J.M. Souil, P. Joulain and E. Gengembre, Experimental and theoretical study of thermal radiation from turbulent diffusion flames to vertical target surfaces, Comb. Sci. Tech., 41 (1984) 69-81.

20 T.A. Brzustowski and E.C. Sommer, Predicting radiant heating from flares, in: American Petroleum Institute, Proc. Div. of Refining, Vol. 53, Washington, D.C., 1973, pp. 865-893.

21 D.M. DeFaveri, G. Fumarola, C. Zonato and G. Ferraiolo, Estimate flare radiation intensity, Hydrocarbon Processing, (May 1985), 89-91.

22 G. Fumarola, D.M. DeFaveri, R. Pastorino and G. Ferraiolo, Determining safety zones for exposure to flare radiation, in: 4th Intl. Symp. Loss Prevention and safety promotion in the process industries, Harrogate, England, Sept. 12-16, 1983, pp. G23-G30.
23 G.T. Kalghatgi, The visible shape and size of a turbulent hydrocarbon diffusion flame in a cross-wind, Combustion and Flame, 52 (1983), 91-106.
24 P.A. Croce and K.S. Mudan, Calculating impacts for large open hydrocarbon fires, Fire Safety J., 11(1986) 99-112.
25 K.S. Mudan, Thermal radiation hazards from hydrocarbon pool fires, Prog. Energy Combust. Sci., 10(1984) 59-80.
26 P.P.K. Raj, Calculations of thermal radiation hazards from LNG fires - a review of the state-of-the-art, in: Proc. Transmission Conference (American Gas Assoc.), St. Louis, Mo., 1977, pp. T135-T148.
27 M. Considine, G.C. Grint and P.L. Holden, Bulk storage of LPG - factors affecting offsite risk, in: The assessment of major hazards (I.Chem.E. Symp. Series No. 71), UK, April 1982, pp. 291-320.
28 A.L. Schneider, Liquefied natural gas spills on water: fire modelling, J. Fire and Flam., 11 (Oct. 1980), 302-313.
29 N.A. Eisenberg in F.P. Lees, vid. 14, pp. 521-522.
30 H.C. Hardee and D.O. Lee, Thermal hazard from propane fireballs, Trans. Planning and Tech., 2 (1973) 121-128.
31 B.R. Williamson and L.R.B. Mann, Thermal hazards from propane (LPG) fireballs, Comb. Sci. Tech., 25(1981) 141-145.
32 A.F. Roberts, Thermal radiation hazards from release of LPG from pressurized storage, Fire Safety J., 4(1981/82) 197-212.
33 T.A. Kletz (1977) in F.P. Lees, vid. 14, pp. 426-427.
34 D.A. Lihou and J.K. Maund, Thermal radiation hazard from fireballs, in: The assessment of major hazards (I.Chem.E. Symp. Series No. 71), UK, April 1982, pp. 191-223.
35 W.P. Crocker and D.H. Napier, Quantification of fire hazards of liquid spills from tank trucks, in: Proc. 4th Technical Seminar on Chemical Spills, Toronto, Ontario, February 10-12, 1987, Sponsored by Environment Canada, pp. 77-113.
36 J.S. Klement and D.H. Napier, Hazard analysis of propane tank car failures in a specific location, in: Proc. 3rd Technical Seminar on Chemical Spills, Montreal, Quebec, February 5-7, 1986, Sponsored by Environment Canada, pp. 81-98.
37 N.H. Juul, Diffuse radiation view factors from differential plane source to sphere, Trans. of ASME: J. Heat Transfer, 101 (August 1979) 558-560.
38 B.T.F. Chung and M.H.N. Naraghi, Some exact solutions for radiation view factors from spheres, AIAA J., 19(8) (August 1981) 1077-1081.
39 W.L. Walls, The BLEVE - Part 1, Fire Command, (May 1979) 22-24.
40 W.L. Walls, The BLEVE - Part 2, Fire Command, (June 1979) 35-37.
41 H. Giesbrecht, K. Hess, W. Leuckel and B. Maurer, Analysis of explosion hazards on spontaneous release of inflammable gases into the atmosphere, Ger. Chem. Eng., 4(1981) 305-314.
42 W.E. Baker, P.A. Cox, P.S. Westine, J.J. Kulesz and R.A. Strehlow, Explosion hazards and evaluation, Elsevier, Amsterdam, 1983, pp. 175-180.
43 Nomenclature of hazard and risk assessment in the process industries, I.Chem. E., Rugby, England, 1985.
44 C.A. McDevitt, F.R. Steward and J.E.S. Venart, What is a BLEVE?, in: Proc. 4th Technical Seminar on Chemical Spills, Toronto, Ontario, February 10-12, 1987, Sponsored by Environment Canada, pp. 137-147.
45 R.C. Reid, Some theories on boiling liquid expanding vapour explosions, Fire, (March 1980), 525-526.
46 J. Manas, BLEVES - their nature and prevention, Fire International, (June-July 1984) 27-39.
47 N.R. Kuloor, D.M. Newitt and J.S. Bateman, Propane, in: F. Din (Ed.), Thermodynamic Functions of Gases, Vol. 2, Butterworths Scientific Publications, London, 1956, pp. 115-145.

48 N.B. Vargaftik, Tables on the Thermophysical Properties of Liquids and Gases: in Normal and Dissociated States, 2nd edn., John Wiley and Sons, Inc., N.Y., 1975, pp. 235-243.
49 M.E. Grimes, Hazardous materials transportation accidents (Fire and Explosion Potential, Serious Threat to Fire Fighters): Topical Information Bullentin No. 1-74, Fire Command!, (April 1974), 11-16.
50 W.E. Martinsen, D.W. Johnson and W.F. Terell, BLEVEs: their causes, effects and prevention, Hydrocarbon Processing, (November 1986) 141-148.
51 B. Maurer, K. Hess, H. Giesbrecht and W. Leuckel, Modelling of vapour cloud dispersion and deflagration after bursting of tanks filled with liquefied gas, in: 2nd Intl. Symp. on Loss Prevention and Safety Promotion in the Process Industries, Heidelberg, Fed. Republic of Germany, Sept. 6-9, 1977, pp. 305-322.
52 D.H. Slater, Vapour clouds, Chem. and Ind., (May 1978) 295-302.
53 W.J. Bradford, Standards on safety: how helpful are they for practising engineers, CEP, (August 1985) 16-18.
54 API Standard 5210, Design and Construction of LP-Gas Installations at Marine and Pipeline Terminals, Natural Gas Processing Plants, Refineries, Petrochemical Plants and Tank Farms, 4th edn., American Petroleum Institute, Refining Dept., Wash., D.C., December 1978, pp. 1-2.
55 NFPA 58 - 1983, Standard for the storage and handling of liquefied gases, National Fire Protection Association, NFC, v. 2 (1985).
56 CAN1-B149.2 - 1976, Installation code for propane burning appliances and equipment, National Standard of Canada, Canadian Gas Association, Don Mills, Canada, 1976, pp. 92-111.
57 Liquefied petroleum gas, Chapter 43, Handbook of Industrial Loss Prevention, 2nd edn., Factory Mutual Engineering Corp., McGraw-Hill Book Co., N.Y., 1967, pp. 43/1-43/15.
58 Institute of Petroleum (UK), Refining safety code, in: C.H. Vervalin (Ed.), Fire Protection Manual for Hydrocarbon Plants, Vol. 2, Gulf Publishing Co., Houston, Texas, 1981, pp. 124-125.